A R C H I V E S O F M E T A L L U R G Y A N D M A T E R I A L S
Volume 58 2013 Issue 2
DOI: 10.2478/amm-2013-0016

T. CZEPPE*, G.F. KORZNIKOVA**, A.W. KORZNIKOV**, L. LITYŃSKA-DOBRZYŃSKA*, Z. ŚWIĄTEK*

MICROSTRUCTURE OF THE NiAlV ALLOYS SUBJECTED TO THE HPT DEFORMATION

MIKROSTRUKTURA STOPÓW NiAlV PODDANYCH ODKSZTAŁCENIU METODĄ SKRĘCANIA POD WYSOKIM CIŚNIENIEM

Some attention in physical metallurgy is devoted to the mechanisms of decomposition of the disordered phases via eutectoid transformation accompanied by the atomic ordering. In case of the non-pearlitic modes of transformation this concerns intermetallic phases of the general description A_3B-A_3C. The application of intensive deformation like HPT may introduce opposite mechanisms introducing some degree of the metastable disordered phase structure at room temperature. The paper presents results of the phase composition and microstructure studies of the alloys of composition $Ni_{75}Al_xV_y$ (where x =15, 10, 5 and y =10, 15, 20), which undergo the solid-state eutectoid decomposition at temperature 1281 K, in the equilibrium conditions. The alloys achieved by the cold crucible levitation method were later intensively deformed with the method of high pressure torsion (HPT). The alloys after HPT revealed homogenous, metastable $L1_2$ (Ni_3Al) structure in place of the eutectoid product $L1_2$-$D0_{22}$. The average size of the Sherrer's coherent diffraction volumes did not exceed 9 nm, suggesting nano-structure of the material. Transmission electron microscopy (TEM) and high resolution electron microscopy (HRTEM) revealed that the micro- and nano- deformation twins were the main feature of the microstructure, dividing volume into cells of the sizes similar to the coherent volumes. The HPT deformation did not influence atomic order. The results are compared with those achieved for the injection cast samples.

Keywords:Ni_3Al, Ni_3V, eutektoid decomposition, microstructure, HPT;

W publikacjach z zakresu fizycznej metalurgii przejawia się zainteresowanie mechanizmami rozpadu, nie perlitycznego typu, faz nieuporządkowanych, zachodzącymi z udziałem uporządkowania atomowego. Dotyczy to faz rodzaju A_3B-A_3C. Zastosowanie intensywnego odkształcenia metodą skręcania pod wysokim ciśnieniem (HPT) może przeciwdziałać rozpadowi wprowadzając fazy metastabilne, o pewnym stopniu nieuporządkowania atomowego, w temperaturze pokojowej. Artykuł przedstawia wyniki badań składu fazowego i mikrostruktury stopów o składzie $Ni_{75}Al_xV_y$ (gdzie x =15, 10, 5 i y =10, 15, 20), podlegających, w warunkach równowagi, rozpadowi eutektoidalnemu w temperaturze 1281 K. Stopy otrzymano metodą lewitacji w zimnym tyglu (CCLM) a następnie poddano przeróbce metodą intensywnego odkształcenia skręcaniem pod wysokim ciśnieniem. Po takim procesie stopy wykazywały jednorodną strukturę $L1_2$ fazy Ni_3Al, zamiast produktów rozpadu eutektoidalnego w postaci struktur $L1_2$ i $D0_{22}$. Średni rozmiar koherentnych obszarów rozpraszania Sherrera nie przekraczał 9 nm, wskazując na materiał o charakterze nano-strukturalnym. Zastosowanie transmisyjnej mikroskopii elektronowej (TEM) i wysokorozdzielczej transmisyjnej mikroskopii elektronowej (HRTEM) pokazało, że bliźniaki odkształcenia o rozmiarach mikro i nano były głównymi elementami mikrostruktury, dzieląc całą objętość na komórki o rozmiarach podobnych do rozmiarów obszarów koherentnego rozpraszania. Metoda HPT nie wpłynęła natomiast na uporządkowanie atomowe. Wyniki porównano z uzyskanymi dla próbek otrzymanych metodą szybkiego chłodzenia przez wtryskiwanie do wlewnicy.

1. Introduction

Intermetallic phases of the A_3B composition, like Ni_3Al, reveal many interesting properties as constructive materials [1]. The NiAlV alloys, of the compositions belonging to the pseudo-binary phase field through the Ni-Al-V ternary phase diagram, connecting, Ni_3Al and Ni_3V phases, at the equilibrium conditions should undergo eutectoid decomposition at temperature 1281 K [2] (Fig. 1). The eutectoid decomposition in this case is associated with the atomic ordering, as both Ni_3Al and Ni_3V phases belong to the highly ordered, densely packed structures, $L1_2$ and $D0_{22}$, with very high degree of coherence at the interfaces [3-5]. Depending on the particular composition and thermal history, such alloys reveal at room temperature characteristic microstructures resulting from the decomposition/ordering path [6]. These may be influenced by the cooling rate and/or further prolonged annealing, which leads to the different lamellar or maze morphology [6]. It was also reported that mechanical properties of decomposed alloys revealing such microstructure, which were investigated in the tensile and tensile creep tests, were very good [7,8].

* INSTITUTE OF METALLURGY AND MATERIALS SCIENCES, POLISH ACADEMY OF SCIENCES, 25 REYMONTA STR. 30-059 KRAKÓW, POLAND
** INSTITUTE OF METALS SUPERPLASTICITY PROBLEMS, RUSSIAN ACADEMY OF SCIENCES, 39 HALTURINA STR. 450001 UFA, RUSSIA

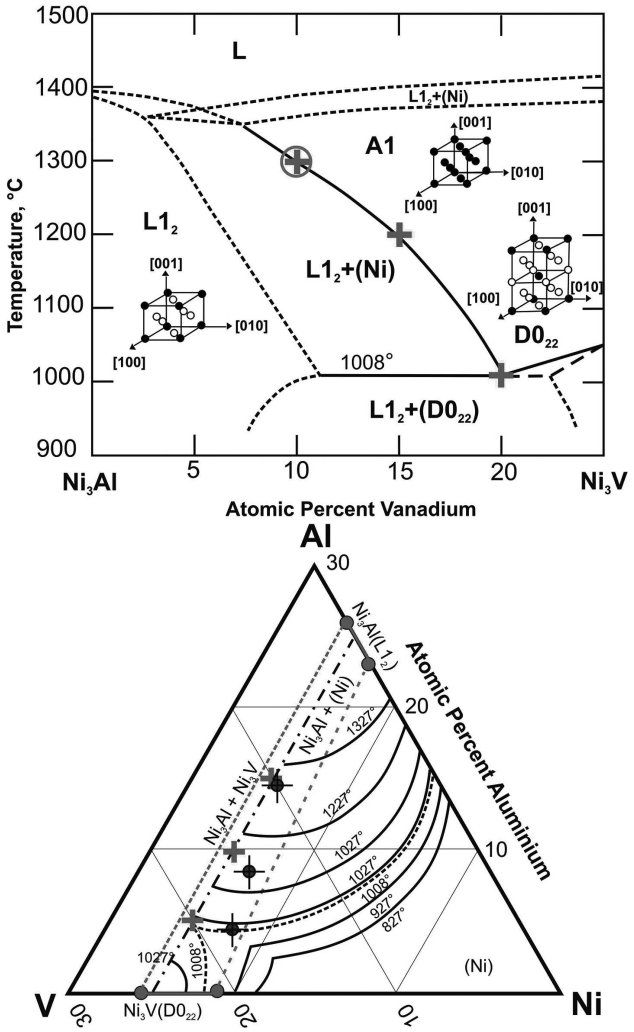

Fig. 1. a) Ni_3Al- Ni_3V section through Ni-Al-V phase diagram [2] with crystallographic structures of the phases and nominal compositions of the investigated alloys, marked by crosses. The experimental composition of the alloy V-1 is marked by circle; b) Location of the nominal and experimental compositions of the alloys is marked on the composition triangle[2] by the crosses and circles respectively. The width of the Ni_3Al and Ni_3V phases fields and hypothetical boundaries between them is shown as straight lines. Assumed 1at% error of the EDS analysis is marked as well

The application of the high pressure torsion to the multi-phase alloys may lead to very different results, to a strong decrease of the grain size down to the nano-microstructure and in some cases, to the metastable phase compositions at room temperature. It may also strongly influence atomic ordering, sometimes much more effectively than rapid quenching [9-11]. In the following sections some basic results presented in literature, concerning ordering in case of Ni_3Al phase and eutectoid decomposition of the coarse grained $Ni_3(Al,V)$ alloys are summarized.

2. Eutectoid decomposition and ordering of the Ni_3 (Al,V) phases

In the case of the hypereutectoid composition the following reaction occurs: Ni(Al,V)SS→Ni_3Al+ Ni(Al,V)SS→Ni_3Al + (Ni_3Al + Ni_3V) [5,6]. At the first stage precipitation of the Ni_3Al phase from the solid solution proceeds together with atomic order solid state reaction: A1 → $L1_2$. The morphology of the primary precipitating phase is cubical [5,6]. The decomposition of the remaining SS into two differently ordered phases: Ni_3Al + Ni_3V, also proceeds with the atomic reordering, having the sequence: A1→$D0_{22}$ →$D0_{22}$+ $L1_2$ →$D0_{22}$ [4,5]. The morphology of the phases may be different, depending on composition and annealing time [4-6].

In the case of the eutectoid composition the following reaction occurs: Ni(Al,V)SS→ Ni_3V→ Ni_3Al + Ni_3V [5,6]. At the first stage disordered A1 structure of SS transforms into the $D0_{22}$ structure of Ni_3V phase [6]. In the next step Ni_3Al phase of the $L1_2$ order precipitates [6]. The morphology consists first of transformation twins followed by formation of the Ni_3Al plates in them [6]. Ageing leads to a maze structure similarly to hypereutectoid compositions [6].

The paper presents results of the investigation of the phase composition and microstructure of the $Ni_{75}Al_xV_y$ (where x =15, 10, 5 and y =10, 15, 20) alloys, of the hypereutectoid and eutectoid compositions after intensive deformation with the use of the high pressure torsion (HPT) method at room temperature.

3. Experimental

The alloys were prepared with cold crucible levitation. The high purity metallic components were melted in the induction coil in the copper concentrator, cooled with water, while pure argon gas was used as an inert gas atmosphere. The solidification of the liquid phase took place directly in the concentrator. The method ensures relatively uniform and fast cooling rate. Resulting samples weighted about 9 grams. The experimental compositions were determined with the EDS method. Two different sets of samples were further prepared. The first one was made by injection casting of the re-melted alloys in the copper mould of 3 mm diameter, and the second by intensive deformation with the high pressure torsion method (HPT). The following parameters were used for the process: pressure 5 GPa and 5 rotations at room temperature.

The nominal and experimental compositions of the alloys are presented in Tab. 1. They also, as marked in Fig. 1a, presenting a pseudo-binary cross-section through the equilibrium Ni-Al-V phase diagram, published by Raghaven [2]. The nominal composition of the alloys may be summarized as $Ni_{75}Al_{25-x}V_x$ where x=10, 15, 20. As shown in Figs. 1a,b the V-1 and V-2 compositions should be located at the two-phase field of Ni_3Al phase and Ni(Al,V) solid solution (SS), at high temperature range. The solid solution should decompose through eutectoid solid state reaction into a mixture of Ni_3Al and Ni_3V phases of different structures below temperature 1281 K. The alloy V-3 close to the eutectoid composition, should decompose in the reaction Ni(Al,V)SS→ Ni_3Al + Ni_3V. The experimental compositions of the V-2 and V-3 alloys deviated from the nominal compositions (Tab. 1). However, as shown in Fg. 1b, they remain in the broad range of the Ni_3Al and Ni_3V phases compositions. The boundary lines determined by width of these phase fields are marked in Fig. 1b.

TABLE 1
Nominal and experimental (EDS) compositions of the investigated alloys

Alloy	Ni (% at.)	Al (% at.)	V (% at.)
V-1	75	15	10
V-1 $_{EDS}$	75.8	14.5	9.7
V-2	75	10	15
V-2 $_{EDS}$	76.8	8.9	14.3
V-3	75	5	20
V-3 $_{EDS}$	77.9	4.4	17.7

The analysis of the chemical composition was performed with EDS. The precision of the EDS method was at least 1 at.%. X-ray diffraction (XRD), electron scanning microscopy, transmission electron microscopy and high resolution transmission electron microscopy (SEM, TEM and HRTEM) were used for determination of the phase composition and microstructure of the samples. The following equipment was used: SEM - Philips XL 30 with EDS system, TEM/HRTEM – TECNAI FEI, G2 FEG/200 kV and XR diffractometer Philips X'Pert in the Bragg-Brentano geometry.

4. Results

A. Samples prepared by injection casting to the cooper mould

First, some results concerning V-1 – V-3 samples cast by the injection to the copper mould, presented in [12] will be summarized for comparison with the results after HPT. XRD revealed that V-1 and V-2 samples contained Ni_3Al phase and Ni(Al,V) SS, while the V-3 sample contained only disordered solid solution, metastable at room temperature. The Ni_3Al phase revealed expected $L1_2$ atomic order. These results were confirmed with the use of TEM. Fig. 2 presents typical microstructure of the alloys V-1 and V-2, consisting of the cubic crystallographic variants of primary precipitates of Ni_3Al phase and Ni(Al,V)SS remaining between them. No further decomposition into lamellar structure of Ni_3Al+Ni_3V was found.

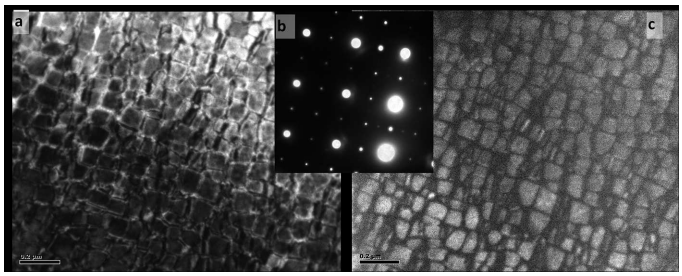

Fig. 2. TEM images of the microstructure of the V-2 sample made by injection casting: a) BF image, b) SADP, orientation [001], note superlattice spots, c) DF image. Different crystallographic variants of Ni_3Al phase of the cubic morphology, retained Ni(Al,V)SS remains between them [12]

B. Samples prepared by high pressure torsion

The samples obtained by HPT are shown in Fig. 3. Their dimensions were: radius R~5 mm and minimal thickness h_{min} 121 μm. From the most common formula for the amount of deformation it follows that maximal deformation was about 730% [13]. The XRD phase analysis (Fig. 4) revealed the homogenous Ni_3Al ($L1_2$) phase composition. As results from the determined values of the lattice parameters a, different from the equilibrium for this phase, the composition, nether containing Ni solid solution nor Ni_3V phase, remains completely metastable, with metastability increasing from V-1 to V-3 alloys, in direction of the eutectoid composition. In this case the $L1_2$ structure has to accommodate additional vanadium atoms. As a result, lattice parameter a increases with the V content from 3.577 to 3.583 Å (±0.002 Å). The other important parameter is the average size of the coherently diffracting domains, which was about 9 nm for all the samples. The presence in the diffractions of the $(100)_{Ni3(Al,V)}$ and $(110)_{Ni3(Al,V)}$ peaks proves that the atomic ordering took place in the samples.

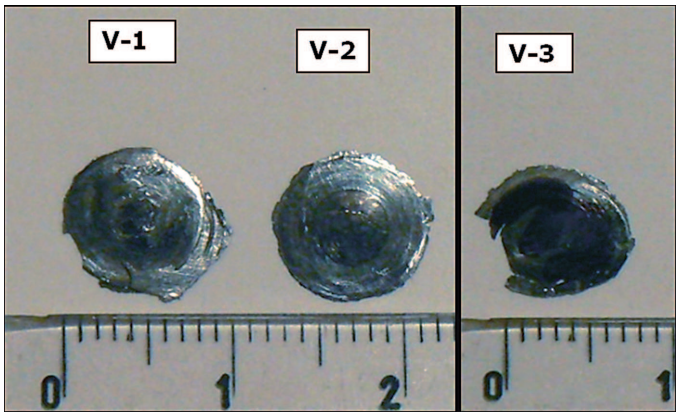

Fig. 3. The samples after intensive deformation with HPT method

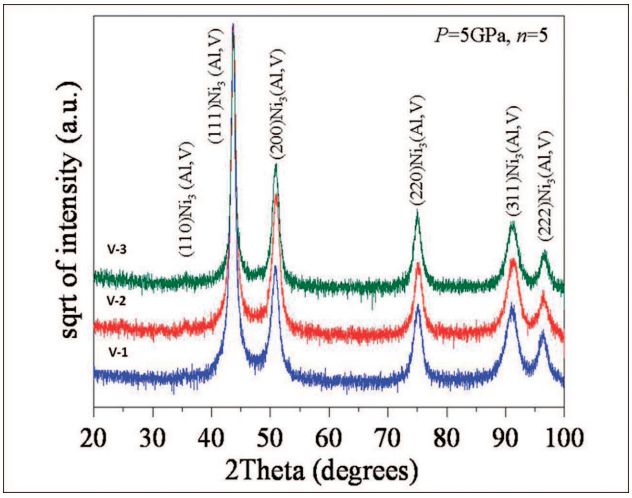

Fig. 4. XRD for the samples V-1, V-2 and V-3 after intensive deformation with HPT. The $L1_2$ structure of Ni_3Al phase is seldom present

The microstructure of the samples V-2 and V-3 were investigated with use of the transmission and high resolution electron microscopy. The bright field (BF) microstructure is shown in Fig. 5a. It reveals high density of disloca-

tions, concentrated also in the so called “deformation poles”. It is not possible to recognize the grain boundaries in such as deformed state. Electron diffraction observed with a large aperture (Fig. 5b) shows the elongated shape of the diffraction spots characteristic of the plastically deformed material. The electron diffraction from the selected area (Fig. 5c) presents [011] orientation of the ordered $L1_2$ structure. The (001) and (011) type spots related to the atomic order are weak but visible.

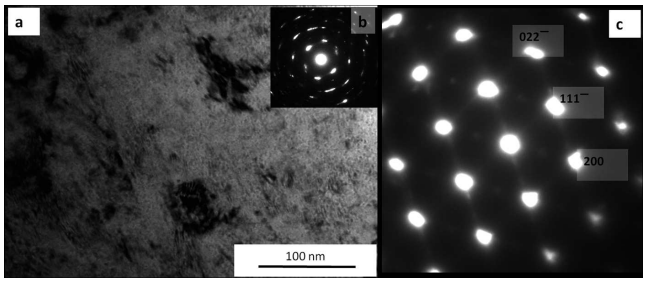

Fig. 5. a) TEM image of the microstructure of V-2 alloy in BF technique. Foil orientation [011]; b) electron diffraction with large aperture typical of the deformed material; c) SADP lattice and superstructure spots of the $L1_2$ structure

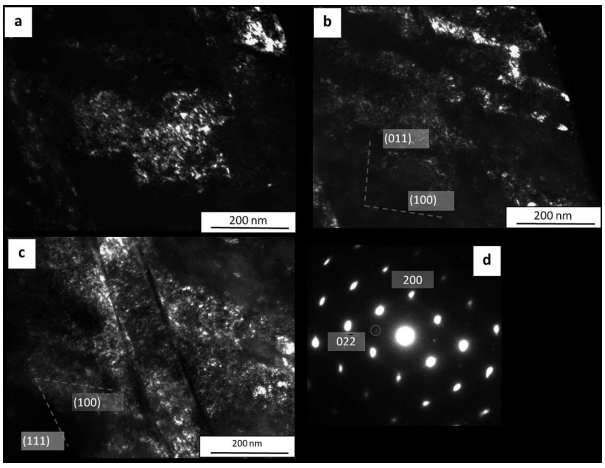

Fig. 6. a, b, c – TEM microstructure in DF, foil orientation [011]; a) ordered domains visible, b, c) deformation twins, traces of the basic crystallographic planes marked; d) SADP, foil orientation [011] showing $L1_2$ superstructure spot (marked)

Domains of atomic ordering are visible in a dark field (DF) technique in Fig. 6a-c. Also deformation twins are well defined in this technique (Fig. 6b,c). The traces of the basic twin planes {001}, {011} and {111} are marked on the micrographs. High resolution image of the microstructure in case of the alloy V-2 is presented in Fig. 7, and the inverse FFT (IFFT) after some filtration (Fig. 7b and 8c) in the Fig. 8a. Magnified selected area marked in Fig. 8a is shown in Fig. 8b. It may be concluded that the HPT deformation leads to the formation of the nano-scale structural defects, stacking faults or nano-twins containing a few crystallographic planes, dividing the whole volume into domains, with relatively homogenous lattice orientation (Fig. 7a, 8a, 8c). Neighboring domains, separated by stacking faults or twins reveal crystallographic disorientation (Fig. 8b). The average size of such domains remains similar to the Sherrer’s coherent diffraction domains, determined with XRD (Fig. 8a).

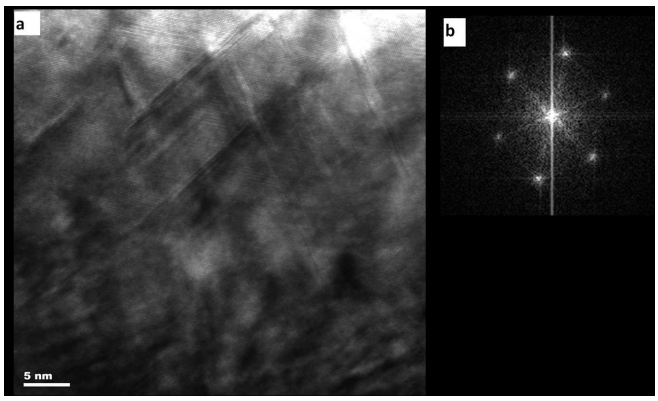

Fig. 7. a) HRTEM image of the microstructure of V-2 alloy after HPT, staking faults or nano-twins visible; b) Fast Fourier Transform (FFT) from the part of the image containing structural faults

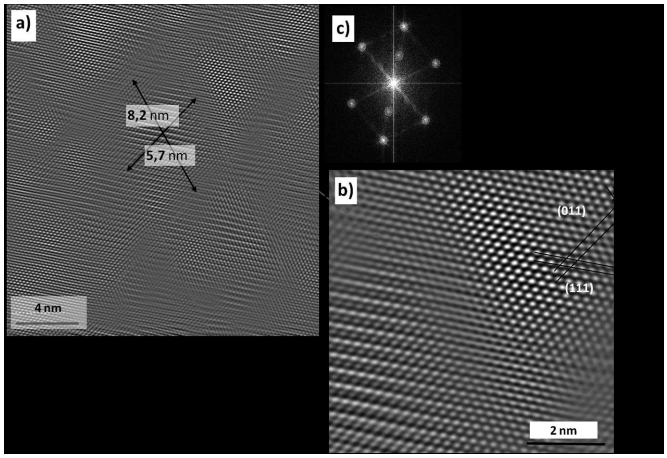

Fig. 8. a) Inverse Fourier Transform (IFFT) from the selected area of the high resolution micrograph after filtration of FFT, the size of the domain with homogenous contrast marked; b) FFT from the marked area, foil orientation [011], $L1_2$ order spots clearly visible as well as weak twin spots; c) enlarged fragment of the a) showing disorientation of the lattice between the bordering domains (only lattice spots used)

The similar TEM and HRTEM investigations results concerning alloy V-3 after HPT processing are presented in Figs. 9, 10 and 11. In Figs. 9a and 10a deformation twins dividing area into separated domains are visible. One set of such twins is bent in the direction of the rotation axis of the anvils. The area of the twin-separated domains reveals high dislocations density (Fig. 10a). The SADP’s in Fig. 9b and 10b also contain weak spots related to the atomically ordered structure. HR images of the V-3 sample presented in Fig. 11 prove, that deformation of the lattice is going mainly through micro- and nano-twin formation. The twinning planes are mostly {111} dense packed planes of $L1_2$ structure of Ni_3Al phase. It is also visible, that the twins contain many stacking faults of different types and that the twins boundaries as well as crystallographic planes are not flat but bent (Fig. 11d, f). This results in an increase in energy of such crystallographic elements of the microstructure.

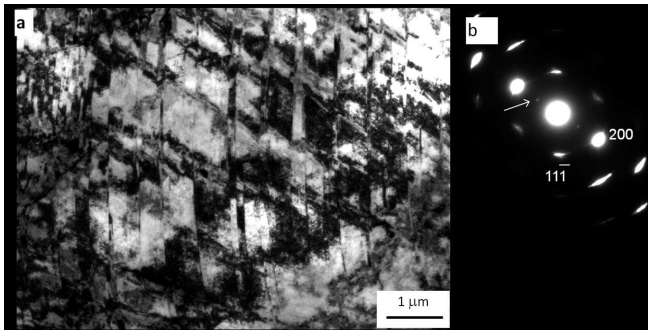

Fig. 9. a) BF microstructure, foil orientation [011]; high concentration of the deformation twins bended in the direction of the rotation axis typical for the HPT deformed samples; b) electron diffraction pattern of the $L1_2$ structure, LRO spots marked, diffraction typical of the deformed material (large aperture)

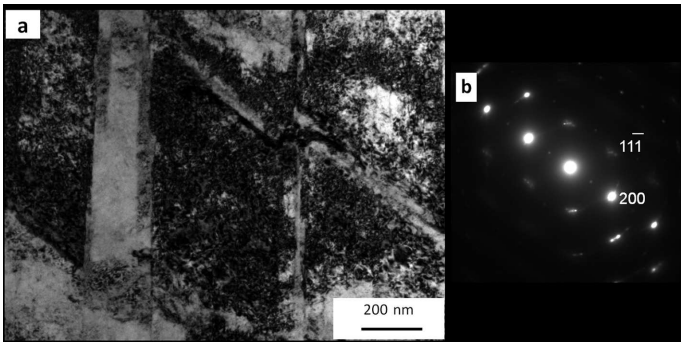

Fig. 10. a) BF microstructure, foil orientation [011]; high concentration of the dislocations between twins; b) electron diffraction pattern, orientation [011]; $L1_2$ LRO spots visible

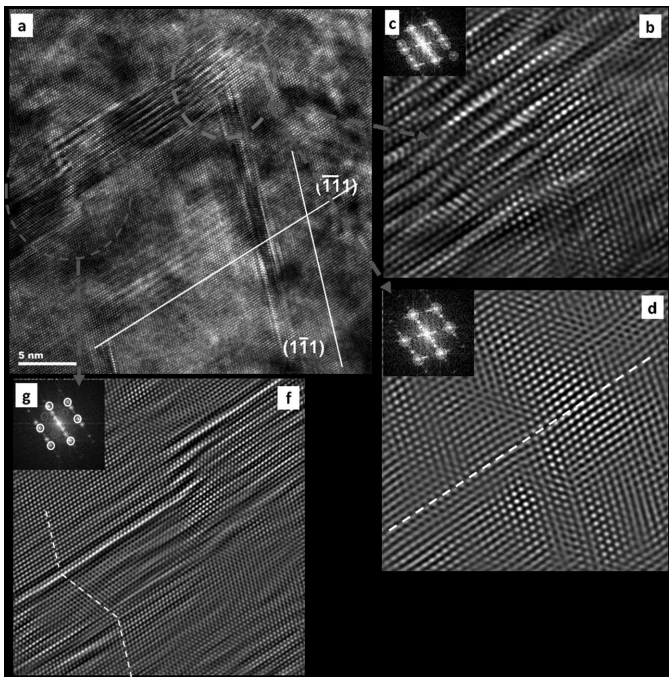

Fig. 11. HRTEM image of the microstructure of V-3 alloy after HPT, foil orientation [011], a) high resolution microstructure; nano-twins containing lattice defects; b, d) magnified IFFT from the marked area in a); b) complicated structural defects in twin visible; c) lattice and twin spots from the FFT used for the IFFT; d) crystallographic planes bent, only lattice spots from the FFT (in e) used; f) nano-twins in the lattice, g) spots for IFFT used

5. Discussion

In difference to the RT equilibrium phase composition of the investigated Ni(Al,V) alloys which should be Ni_3Al+(Ni_3Al+Ni_3V), or to high temperature compositions achieved by injection casting, Ni_3Al+Ni(Al,V)SS, HPT intensive deformation in all the samples introduced homogenous Ni_3Al phase, metastable at RT. However, in applied parameters of HPT, no influence of the method on the atomic $L1_2$ order was noticed. Apart from the homogeneity of the phase composition, the main observed microstructural effect of the deformation was the high density of stacking faults and deformation twins introduced, from micro- to the nano-scale, which divided the samples volume into disoriented neighboring domains. The other, rather obvious observation was the high density of the dislocations in such domains and different stacking faults inside the twins. Also, the twins' boundaries revealed some bending and rather complicated microstructure, suggesting some energetically non-equilibrium state of the elements of microstructure [14]. The Sherrer's coherent domains, about 9 nm in average size, allow the qualification of the HPT samples as a nanomaterial. All the observations connecting deformation mechanism predominantly through the micro-twins formation remain in complete agreement with the papers presenting microstructure of the Ni_3Al phase after intensive deformation with the HPT method [14]. The main difference to the presented results is that in some reported experiments, HPT deformation lead to the complete disordering of the alloy [11], which was not the case in the results presented above.

6. Conclusions

1. Intensive deformation with the HPT of the $Ni_{75}Al_xV_y$ alloys (where x = 15, 10, 5 and y = 10, 15, 20) leads to the metastable, homogenous $L1_2$ structure of Ni_3Al phase in place of the eutectoid decomposition into Ni_3Al + Ni_3V phases, of $L1_2$ and $D0_{22}$ structures.
2. Microstructure after HPT deformation consists mainly of the stacking faults and micro- and nano-twins formed on the {111}densely packed planes. It reveals also very high density of dislocations and metastable, non-planar twin boundaries.
3. The coherent volume remained of the average size 9 nm. The grains boundaries after HPT can not be determined without annealing.
4. In difference to the structures achieved by the rapid solidification and ball milling, the HPT deformation with applied parameters does not seem to influence $L1_2$ atomic order.

Acknowledgements

- The work was financed by the Research Program of IMMS PAS Krakow, as the project Nr Z-10 in 2008-2011 years;
- The work was realized as part of the cooperation between IMMS PAS Krakow – Inst. of Metals Superplasticity RAS Ufa in the project " The influence of the intensive deformation on the structure and physical properties of Ni-based intermetallic phases of closed packed structures and amorphous phases", under the agreement on scientific cooperation between PAS and RAS;

- The experimental part was performed in the PAC accredited Laboratories of IMMS PAS.

REFERENCES

[1] D.B. Miracle, Acta Metal Mater. **41**, 649 (1993).
[2] V. Raghaven, J Phase Equlib. **26**, 273 (2005).
[3] A.K. Sinha, Trans TMS-AIME **245**, 911 (1969).
[4] Y. Nunomura, Y. Kaneno, H. Tsuda, T. Takasugi, Acta Mat **54**, 851 (2006).
[5] S. Shibuya, Y. Kaneno, M. Yoshida, T. Shishido, T. Takasugi, Intermetallics **15**, 338 (2007).
[6] M. Takeyama, M. Kikuchi, Intermetallics **6**, 573 (1998).
[7] S. Shibuya, Y. Kaneno, M. Yoshida, T. Shishido, T. Takasugi, Acta Mat **54**, 861 (2006).
[8] S. Shibuya, Y. Kaneno, M. Yoshida, T. Shishido, T. Takasugi, Intermetallics **15**, 119 (2007).
[9] A.M. Barros, J.A.S. Tenório, Intermetallics **13**, 137-140 (2005).
[10] M.D. Baro, J. Mlagelada, S. Surinach, N. Clavaguera, N.T. Clavaguera-Mora, in: Ordering and disordering in alloys, ed. A .R. Yavari, Elsevier Applied Science, 55-66 (1992).
[11] A.V. Korznikov, O. Dimitrov, G.F. Korznikiova, J.P. Dallas, S.R. Idrisova, R.Z. Valiev, F. Faudot, Acta Mater **47**, 3301 (1999).
[12] T. Czeppe, G. Korznikova, Z. Świątek, A. Sypień, A. Korznikova, W. Krajewski, Solid State Phenom. **172-174**, 475-480 (2011).
[13] M.H. Shorshorov, A.V. Korznikov, Materialovedenie **6**, 8 (2002).
[14] Ju.R. Kolobov, R.Z. Valiev, G.P. Grabovecka-ia, A.P. Żiliaev, E.F. Dudaev, H.V. Ivanov, M.B. Ivanov, O.A. Kaszin, E.V. Naidenkin, Zernogranicznaia diffuzia i svoistva nanstrukturnych materialow, eds. Ju.R. Kolobov, R.Z. Valiev; 'Nauka' 2001 (russ.), pp. 20-23.

Received: 20 January 2013.